Technical University of Denmark

DTU

EPR experiments in LiTbF4, LiHoF4, and LiErF4 at submillimeter frequencies

Magariño, J.; Tuchendler, J.; Beauvillain, P.; Laursen, Ib

Link back to DTU Orbit

DTU Library
Technical Information Center of Denmark

EPR experiments in LiTbF$_4$, LiHoF$_4$, and LiErF$_4$ at submillimeter frequencies

J. Magariño and J. Tuchendler*

Laboratoire de Physique des Solides de l'Ecole Normale Superieure,[†] 24 rue Lhomond, 75231 Paris, France

P. Beauvillain

Institut d'Electronique Fondamentale,[†] Batiment 220, Université Paris Sud, 91405 Orsay, France

I. Laursen

Department of Electrophysics, The Technical University of Denmark: DK 2800, Lyngby, Denmark
(Received 12 March 1979)

Electron-paramagnetic-resonance experiments in LiTbF$_4$, LiHoF$_4$, and LiErF$_4$ have been performed at frequencies between 70 and 600 GHz, in magnetic fields up to 60 kG and in the temperature range $1.4 < T < 25$ K. The experiments yield precise information on the lowest levels of the rare-earth ions. We investigated the resonance line position and the linewidth as a function of frequency and temperature. The g values and the couplings between the lowest levels are determined. The local field around the magnetic ion is measured directly and the Curie constant Θ_C can be calculated. The results give the single-ion parameters appropriate to a description of the low-temperature magnetism in these compounds.

I. INTRODUCTION

The LiY$_{1-x}R_x$F$_4$ series, where R is a rare earth, have attracted considerable interest primarily because they are efficient laser host materials.[1]

In the dilute materials, LiY$_{1-x}R_x$F$_4$, Sattler and Nemarich[2] have observed the EPR spectra of Nd^{3+}, Dy^{3+}, Er^{3+}, and Yb^{3+}. The Tb^{3+} spectrum has been observed by Laursen and Holmes[3] and the Ho^{3+} spectrum by Magariño et al.[4]

The magnetic properties of the LiRF$_4$ compounds also present a great theoretical interest due to the simplicity of these materials. They consist of fairly ionic atoms with high-point tetragonal symmetry (S_4), the rare earths being primarily coupled through dipolar forces.

The magnetic properties of LiTbF$_4$ have first been observed by Holmes et al.[5] by magnetic-susceptibility measurements. They showed that LiTbF$_4$ is ferromagnetic below $T_C = 2.86$ K with the magnetic moment along the tetragonal $\vec{c}$ axis, and that the predominant contribution to the Curie-Weiss temperature, Θ_C, comes from the dipolar forces. The precise comparison between dipolar and exchange interaction has been made by quasielastic-neutron-scattering experiments.[6] It confirmed that the dipolar interactions are more important than the exchange interactions.

LiHoF$_4$ and LiErF$_4$ have been studied by Hansen et al.[7] Their magnetic-susceptibility measurements showed that LiHoF$_4$ is ferromagnetic, with the magnetic moment along the $\vec{c}$ axis. No ordering was observed in LiErF$_4$ which was predicted by these authors to be ferromagnetic. The crystal-field parameters were determined in the two materials. The ferromagnetism in LiHoF$_4$ has also been studied by Cooke et al.[8] which determined the transition temperature $T_C = 1.53$ K. The magnetic interactions are similar to LiTbF$_4$, the dipolar interactions being predominant.

The magnetic susceptibility in LiErF$_4$ was studied by Beauvillain et al.[9] at ^{3}He temperatures: LiErF$_4$ is antiferromagnetic, $T_N = 0.38$ K and the magnetic moments are perpendicular to the $\vec{c}$ axis in agreement with the theoretical prediction of Misra and Felsteiner.[10] Beauvillain et al.[11] have recently studied LiDyF$_4$, which shows properties similar to LiErF$_4$, with $T_N = 0.581 \pm 0.05$ K.

The optical absorption spectra of LiTbF$_4$, LiHoF$_4$, and LiErF$_4$ have been studied by Christensen[12,13] and the crystal-field parameters have been determined.

The singular properties of LiTbF$_4$ and LiHoF$_4$ which are good models of dipolar uniaxial ferromagnets are very important for the study of critical phenomena. For Ising dipolar ferromagnets at $d = 3$, the critical behavior can be calculated exactly[14,15] and apart from logarithmic corrections, the classical Landau theory of second-order phase transitions can be applied.

The critical properties of LiTbF$_4$ have been studied by specific-heat,[16,17] neutron scattering,[18-20] and optical[21] measurements. For LiHoF$_4$ the critical properties have been analyzed by susceptibility measurements.[22,23]

We report here, EPR experiments at millimeter and submillimeter frequencies $70 < \nu < 600$ GHz and

in magnetic fields up to 60 kG in LiTbF$_4$, LiHoF$_4$, and LiErF$_4$. The resonances between the lowest levels have been observed for the three compounds. The temperature dependence of the linewidths has been studied for LiTbF$_4$ and LiHoF$_4$. Resonances due to rare earths and other (iron) residual impurities are also observed but are not analyzed here. EPR experiments on these crystals give information on the crystal-field parameters by the observation of the position in field and by the linewidth dependences of the resonance lines with respect to frequency and temperature. They also give information on the magnetic parameters by the direct observation of the internal fields in the crystal which produce shifts in the resonance positions. These results give the parameters which are necessary for a detailed description of the magnetism in LiTbF$_4$, LiHoF$_4$, and LiErF$_4$ and for the critical properties of these compounds. We reported earlier some preliminary results.[24]

The LiTbF$_4$, LiHoF$_4$, and LiErF$_4$ samples used in this study were single crystals grown by Hansen and Laursen by a hydrofluorination method described in Ref. 3. Either spheres or parallelepipeds were used.

The microwave and cryogenic setups have been described elsewhere.[4]

II. EXPERIMENTAL RESULTS AND INTERPRETATION

A. LiTbF$_4$

Two single crystals were used, one parallelipedic (sample 1) the other spherical (sample 2). Only one resonance signal due to the Tb^{3+} ions was observed in the whole range of frequencies and temperatures. The resonance line was broad at low frequencies (70 < ν < 135 GHz) and narrowed as the frequencies increased. Figure 1 shows recorder traces taken at different frequencies at $T = 4.2$ K for sample 1. The hyperfine structure from the 100% abundant isotope ^{159}Tb with nuclear spin $I = \frac{3}{2}$ consists of four equally spaced resonances lines. It was only resolved for sample 2, and only at the highest frequencies (Fig. 2). The spacing between the hyperfince resonance lines is $A = 250 \pm 5$ Gauss for $\vec{H} \parallel \vec{c}$ in agreement with the values obtained for the dilute material by some of the present authors,[25] $A = 252 \pm 5$ Gauss, and by Laursen and Holmes, $A = 252.9 \pm 0.5$ Gauss.[3]

The angular dependence of the resonance line in the (c,a) plane, shown on Fig. 3. displays a very large anisotropy and confirms the Ising behavior. Figure 4 shows the frequency dependence at 4.2 K of the resonance line as a function of the magnetic field. These frequency field dependences of the resonance signal for $\vec{H} \parallel \vec{c}$ have been also studied at $T \leq 1.5$ K in the ferromagnetic phase. At high frequencies
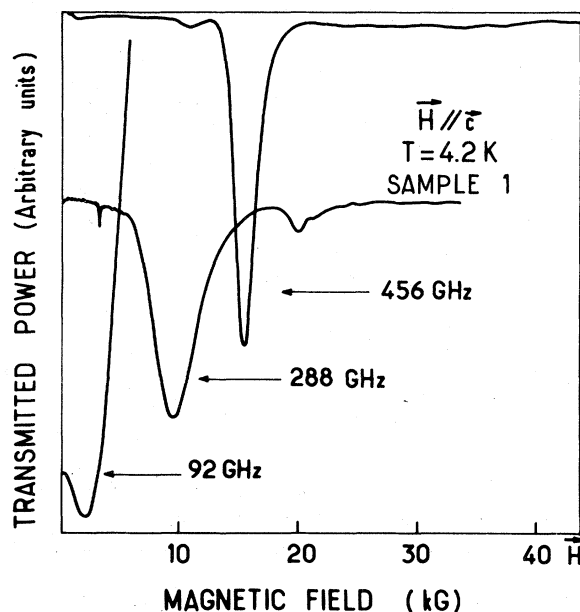

FIG. 1. Recorder traces at three frequencies for sample 1 of LiTbF$_4$. The small resonances observed are due to impurities.
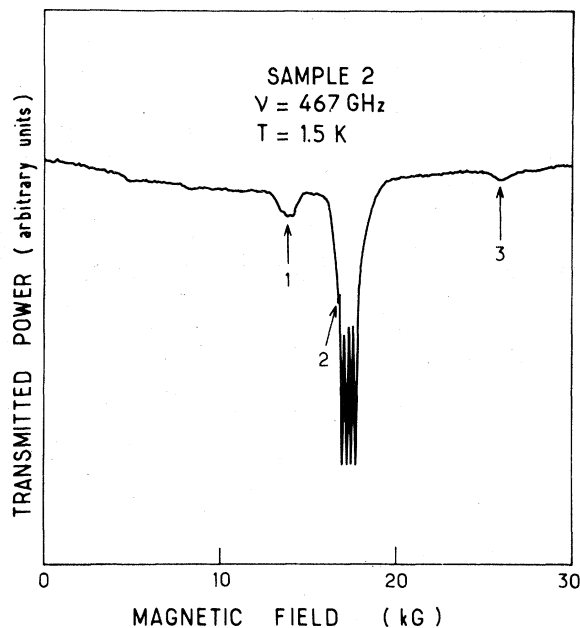

FIG. 2. Recorder traces at 467 GHz for sample 2 of LiTbF$_4$. Resonance 1 and 3 are produced by impurities. Resonance 2 is a forbidden hyperfine transition.
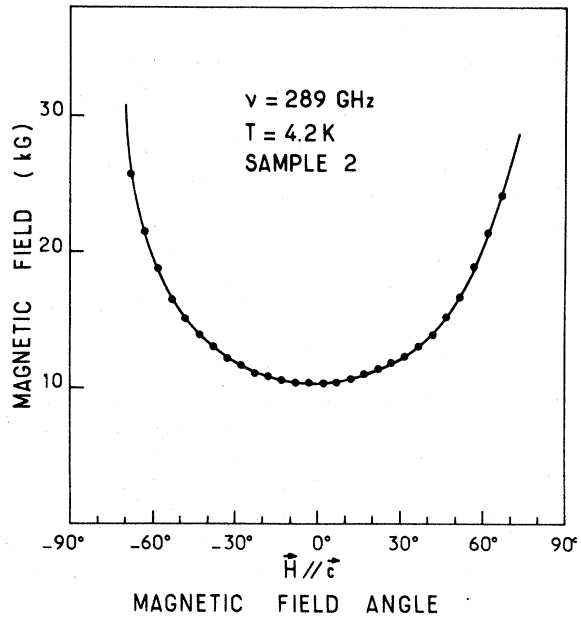
FIG. 3. Angular dependence of the main resonance at 289 GHz for $\vec{H}$ in a (c,a) plane in LiTbF$_4$ (sample 2). Dots, experiment; continuous line, a guide to the eye.
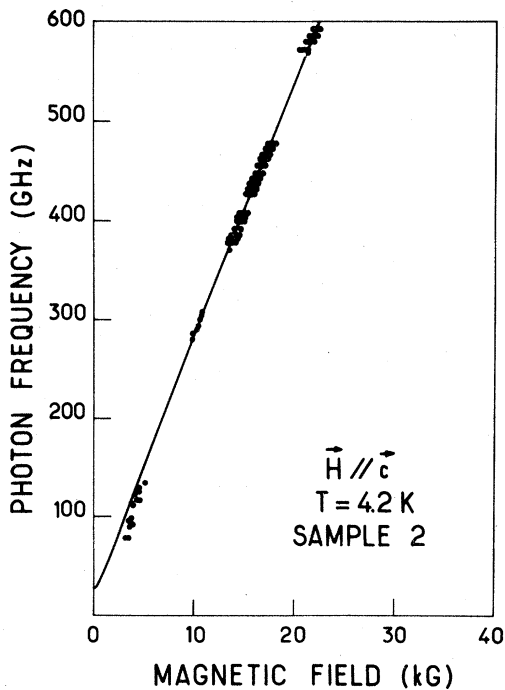
$(\nu > 135$ GHz) for which the sample is saturated, the experimental results are similar to those obtained at $T = 4.2$ K. At low frequencies $(70 < \nu < 135$ GHz), attempts to observe more clearly the ferromagnetic resonance were unsuccessful. This is probably due to the existence of domains below T_C.[8]

Figure 5 shows the temperature dependence of the linewidth of the resonance line for two different frequencies in the temperature range $1.4 < T < 25$ K for sample 2.

In a crystal field of S_4 symmetry, the $(2J + 1)$fold degenerate ground term $^7F_6$ of the non-Kramers Tb^{3+} ion $(4f^8)$ splits into 10 levels (3 doublets and 7 singlets),

$$^7F_6 \rightarrow 3\Gamma_1 + 4\Gamma_2 + 3\Gamma_{3,4} \ .$$

The $\Gamma_{3,4}$ doublets correspond to pairs of singlet representations. The optical measurements of Ref. 12 shows that the two lowest levels for two Γ_2 singlets approximately 2 cm^{-1} apart. The other levels are at 100 cm^{-1} above.

The corresponding wave functions of these two levels have the general form

$$|\Gamma_2^i\rangle = \alpha_i(e^{J\phi_i}|+6\rangle - e^{-J\phi_i}|-6\rangle)$$

$$+ \beta_i(e^{Jx_i}|+2\rangle - e^{-Jx_i}|-2\rangle) \ . \tag{1}$$

The large experimental value $g_Z = 17.85$ (see below) suggests that these wave functions are made up mainly of $|J_Z\rangle = \pm 6$ states.

The magnetic field dependence for $\vec{H} \parallel \vec{c}$ of these levels can be obtained from the effective spin Hamil-

FIG. 4. Frequency vs magnetic field of the resonance for $\vec{H} \parallel \vec{c}$ in LiTbF$_4$ (sample 2). Dots, experiment; continuous line, theory.
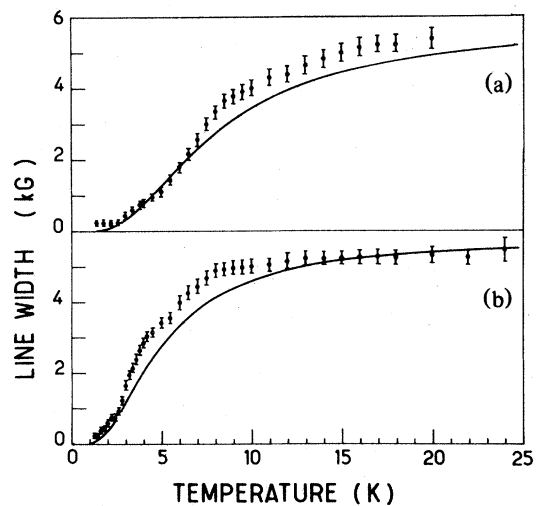

FIG. 5. Linewidth vs temperature of the resonance for $\vec{H} \parallel \vec{c}$ in LiTbF$_4$ (sample 2). (a) $\nu = 456.5$ GHz. (b) $\nu = 285$ GHz. Dots, experiment; continuous line, theory.

tonian with $S = \frac{1}{2}$,[3]

$$\mathcal{H} = g_Z\mu_B H_Z S_Z + \Delta S_x + A S_Z I_Z \ , \qquad (2)$$

where Δ is the zero-field splitting of the two Γ_2 levels and A is the hyperfine constant.

The energy levels are given by

$$E(m_s, m_I) = m_s[(g_Z\mu_B H_Z + A m_I)^2 + \Delta^2]^{1/2} \ , \qquad (3)$$

where $m_s = \pm\frac{1}{2}$ and $m_I = \pm\frac{3}{2}, \pm\frac{1}{2}$.

The transitions induced by a microwave field $\Delta m_s = 1$, $\Delta m_I = 0$ are given by

$$h\nu = [(g_Z\mu_B H_Z + A m_I)^2 + \Delta^2]^{1/2} \ , \qquad (4)$$

where H_Z is the local magnetic field related to the external magnetic field, H_{0z} by the relation

$$H_Z = H_{0z} + (\lambda - 4\pi N_c/V)M_Z \ , \qquad (5)$$

where λ is the molecular-field constant, N_c is the demagnetizing factor, V is the gram ionic volume, and M is the magnetization which depends on the temperature, and implicitly depends on the local field via the expression

$$\frac{M_Z}{M_0} = \frac{g_Z\mu_B H_Z}{[(g_Z\mu_B H_Z)^2 + \Delta^2]^{1/2}}$$

$$\times \tanh\left[\frac{1}{2kT}[(g_Z\mu_B H_Z)^2 + \Delta^2]^{1/2}\right] \ . \qquad (6)$$

M_0 is the saturation magnetization. The hyperfine structure is neglected for simplicity. In expression (5), the λ constant contains only the dipolar contribution when the spins contribute to the same hyper-

fine signal, and the dipolar and exchange contributions when the spins contribute to different hyperfine signals.[26-28] As the material is primarily dipolar coupled, the λ constant has practically the same value as the molecular-field constant obtained from susceptibility experiments. The Curie temperature Θ_C can be determined from the value of the molecular-field constant λ according to

$$\Theta_C = \frac{g_Z\mu_B}{2k}\lambda M_0 \ . \qquad (7)$$

The best-fit values for the parameters of the spin Hamiltonian (2) and for the Curie temperature are given for the two samples used in Table I where they are compared with other experimental results. The low-temperature ferromagnetism in LiTbF$_4$ is described using a fundamental doublet with $g_Z = 17.85 \pm 0.1$ and $g_x = g_y = 0$. The Ising behavior is a consequence of this anisotropy of the g factor. The dipolar contribution to the Curie constant is predominant.[5,6,24] The splitting Δ measured directly in our experiment is the parameter which determines the validity of application of the Ising model. We find $\Delta = 30 \pm 10$ GHz which is close to the value found in LiYF$_4$:Tb^{3+}.[25] The experimental error is large. It is a consequence of the poor precision in the line position due to the large linewidth in the low-frequency region ($70 < \nu < 135$ GHz). The ratio $\Delta/kT_C = 0.50$, $T_C = 2.86$ K, is an important parameter for a detailed description of the system, the critical parameters being possibly affected by a finite Δ/kT_C ratio.[19]

The frequency and temperature dependences of the linewidth have been analyzed in terms of the line

TABLE I. Values for the best-fit parameters obtained in LiTbF$_4$ from the frequency dependence of the resonance line. The values of several of these parameters obtained from other works (see Refs. 3, 5, and 6) are included for comparison.

	g_Z	$\left(\lambda - \dfrac{4\pi}{V}N_c\right)M_0$ (kG)	Δ (GHz)	$\dfrac{4\pi}{3}N_c$	Θ_C (K)
Sample 1	17.85 ± 0.1	2.5 ± 0.1	30	$4\pi \times 0.24$	3.55 ± 0.1
Sample 2	17.85 ± 0.1	1.3 ± 0.1	30	$4\pi/3$	3.58 ± 0.1
LiYF$_4$:Tb^{3+}	17.85 ± 0.1	$\cdots$	28 ± 2	$\cdots$	$\cdots$
LiYF$_4$:Tb^{3+} Ref. 3	17.7 ± 0.2	$\cdots$	27.98 ± 0.06	$\cdots$	$\cdots$
Susceptibility Ref. 5	17.8	$\cdots$	$\cdots$	$\cdots$	3.6 ± 0.1
Neutrons Ref. 6	$\cdots$	$\cdots$	$\cdots$	$\cdots$	3.55 ± 0.3

moments theory developed by Kambe and Usui[26] and McMillan and Opechowski.[27] Precise experiments of these dependences have been performed by Svare and Seidel[28] on $Nd(C_2H_5SO_4)_3 \cdot 9H_2O$, $NiSiF_6 \cdot 2H_2O$, and $K_2Cu(SO_4)_2 \cdot 6H_2O$.

According to these theories, the second moment of the resonance line is

$$h^2 \langle \nu^2 \rangle = \frac{\text{Tr}\{b(\tilde{\mathcal{H}})[(M_-,\tilde{\mathcal{H}}),(\tilde{\mathcal{H}},M_+)]\}}{\text{Tr}[b(\tilde{\mathcal{H}})(M_-,M_+)]} , \quad (8)$$

where $\tilde{\mathcal{H}}$ is the truncated Hamiltonian[26] and the operators M_+ and M_- are defined by

$$\langle n|M_+|n'\rangle = \begin{cases} \langle n|M|n'\rangle , & E_n' < E_n \\ 0 , & \text{otherwise} , \end{cases}$$

$$\langle n|M_-|n'\rangle = \begin{cases} \langle n|M|n'\rangle , & E_n' < E_n \\ 0 , & \text{otherwise} . \end{cases}$$

E_n are the energies of the unperturbed spin system, M the truncated-microwave-field operator[26] and $b(x)$ the Boltzmann factors $e^{-x/kT}$.

For LiTbF$_4$, we suppose for simplicity $\Delta = 0$. The second central moment is then given through the expression[28]

$$(h^2 \langle \Delta \nu^2 \rangle)_c = (16N)^{-1}(2g_Z^2 + g_\perp^2)\mu_B^4$$

$$\times [1 - \tanh^2(g_Z \mu_B H_Z / 2kT)]$$

$$\times \sum_{i,j} \left[\frac{1 - 3\cos^2\theta_{ij}}{r_{ij}^3} \right]^2 . \quad (9)$$

We have fitted the temperature dependence of the linewidths in Fig. 5 by the expression

$$\Delta H = A[1 - \tanh^2(g_Z \mu_B H_Z / 2kT)]^{1/2} , \quad (10)$$

with $A = 5.75$ kG in good agreement with the value calculated from Eq. (9), $A = 6.5$ kG. The calculated curves in Fig. 5 describe qualitatively the observed temperature dependence.

B. LiHoF$_4$

Three single crystals of LiHoF$_4$ have been studied. The first two crystals were parallelepipeds (samples 1 and 2) and the third was a sphere.

At a given frequency we observe, in general, several strong resonances. Some of these resonances have a well resolved hyperfine structure consisting of eight resonance lines due to the 100% abundant isotope ^{165}Ho, with nuclear spin $I = \frac{7}{2}$. The spacing between the hyperfine resonance lines is $A = 474 \pm 10$ Gauss for $\vec{H} \parallel \vec{c}$ in agreement with the value observed in the dilute material $A = 479 \pm 7$ Gauss.[4]

The angular dependences of the resonance lines

were studied in the (c,a) plane and were similar to those observed in the dilute material.[25]

Figures 6 and 7 show the frequency dependence of the observed resonances as a function of the magnetic field respectively along and perpendicular to the $\vec{c}$ axis. On Fig. 6, note that one resonance extrapolates linearly to zero frequency at zero magnetic field. This is characteristic of transitions between the levels of a doublet. Several other lines extrapolate at 220 GHz and consequently correspond to transitions between this ground-state doublet and another level at 220 GHz above it. One line extrapolates at about 694 GHz and corresponds to a third level at 694 GHz. Another resonance which extrapolates for zero magnetic field at 220 GHz is observed, the frequency of this resonance is almost exactly at a given field the sum of the frequencies of the resonance lines noted $1 \leftrightarrow 2$ and $1 \leftrightarrow 3$ on Fig. 6 for the same value of the field.

Figure 8 shows the temperature dependence of the linewidth of $1 \leftrightarrow 2$ for sample 3 in the temperature range $1.4 < T < 15$ K.
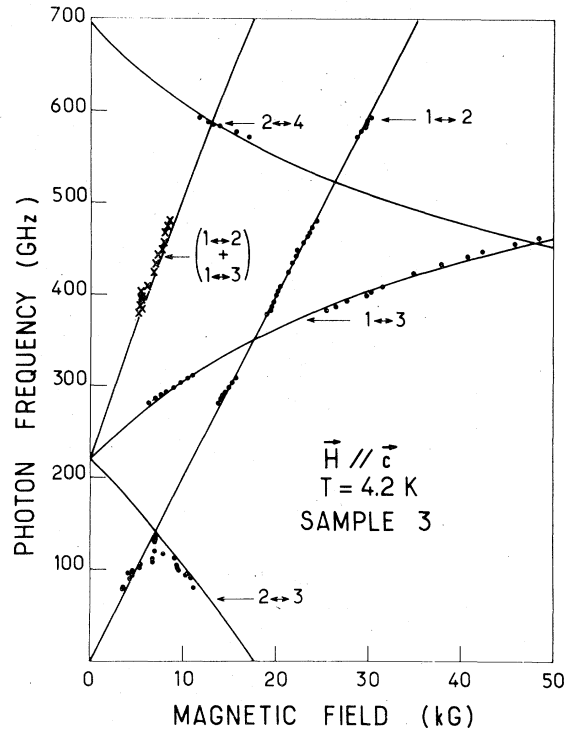

FIG. 6. Frequency vs magnetic field of the resonances for $\vec{H} \parallel \vec{c}$ in LiHoF$_4$ (sample 3). Resonance $1 \leftrightarrow 2$ indicates the transition between the two levels of the fundamental doublet. Resonances $1 \leftrightarrow 3, 2 \leftrightarrow 3$ indicate transitions between these two levels and the first excited state and resonance $2 \leftrightarrow 4$ indicates a transition between a level of the fundamental doublet and a second excited state. Dots, experiment; continuous line, theory.
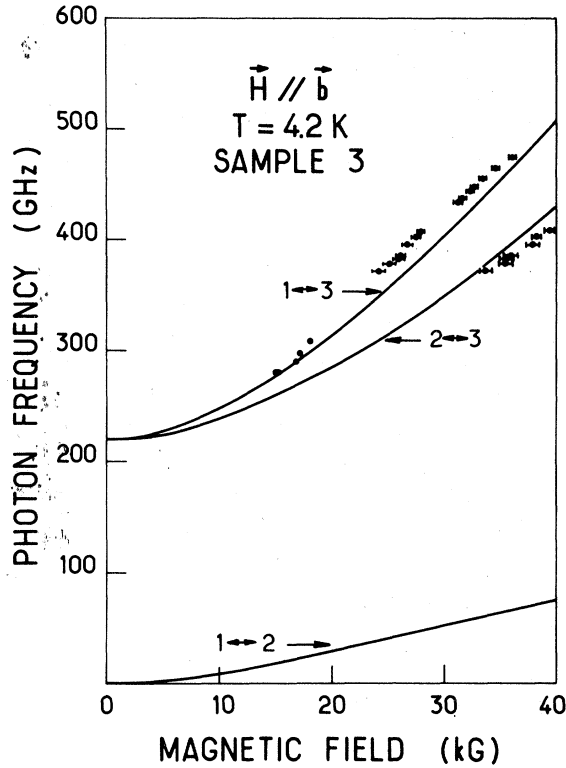
FIG. 7. Frequency vs magnetic field of the resonances for $\vec{H} \parallel \vec{b}$ in LiHoF$_4$ (sample 3). The resonances are indicated with the same notation as in Fig. 6. Dots, experiment; continuous line, theory.

For other transitions, a careful study of the linewidth dependence cannot be made because of the larger linewidths.

These results can be explained as follows. The $2J + 1$ manyfold $^5I_8$ of the non-Kramers Ho^{3+} ion $(4f^{10})$ is split into 13 levels (nine singlets and four
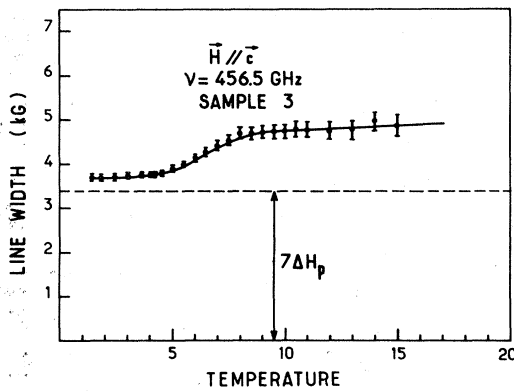

FIG. 8. Linewidth vs temperature of the $1 \leftrightarrow 2$ resonance for $\vec{H} \parallel \vec{c}$ at $\nu = 456.5$ GHz in LiHoF$_4$ (sample 3). The value $7\Delta H_p$ measures the spacing in field between the first and the eighth hyperfine signal. Dots, experiment; continuous line, a guide to the eye.

doublets).

$$^5I_8 \rightarrow 5\Gamma_1 + 4\Gamma_2 + 4\Gamma_{3,4}$$

Optical[8,13] and susceptibility[7,8] measurements show that the lowest level is a $\Gamma_{3,4}$ doublet and the first two excited levels are two Γ_2 singlets.

The magnetic field dependence of these levels can be obtained from the Zeeman Hamiltonian

$$H_Z = g_J \mu_B \vec{H} \cdot \vec{J} \tag{11}$$

and from the knowledge of the wave functions of the levels. The Landé factor g_J for $^5I_8$ is equal to $\frac{5}{4}$. More precisely, the energy levels in presence of a magnetic field are calculated from the diagonalization of the secular equation

$$\det(E_{kl} + \langle \Gamma^k | H_z | \Gamma^l \rangle - \lambda \delta_{kl}) = 0 \quad , \tag{12}$$

where $k = 1, \ldots, 4$, $| \Gamma^k \rangle$ indicates the k level, $E_{kl} = 0$ if $k \neq l$ and E_{kk} is the energy of the k level at $H = 0$. We consider only the four lowest levels. The general structure of the wave functions of these levels is

$$| \Gamma_{3,4} \rangle = \alpha_1 e^{\pm \beta_1 J} | \pm 7 \rangle + \alpha_2 e^{\pm \beta_2 J} | \pm 3 \rangle$$
$$+ \alpha_3 e^{\pm \beta_3 J} | \mp 1 \rangle + \alpha_4 e^{\pm \beta_4 J} | \mp 5 \rangle \quad ,$$

$$| \Gamma_2^i \rangle = \beta_i (e^{J\phi_i} | +6 \rangle - e^{-J\phi_i} | -6 \rangle)$$
$$\tag{13}$$
$$+ \gamma_i (e^{J\chi_i} | +2 \rangle - e^{-J\chi_i} | -2 \rangle) \quad ,$$

where α_i, β_i, and γ_i are real numbers and $i = 1, 2$.

The study of the transitions between these levels is similar to the case of Ho^{3+} in the diluted material LiYF$_4$:Ho^{3+}.[4] As for LiTbF$_3$, the resonances are shifted by the local magnetic field according to Eq. (5), where the magnetization per ion takes into account the four lowest levels only. For $\vec{H} \parallel \vec{c}$

$$M_z = \frac{\sum_i \mu_i e^{-E_i/kT}}{\sum_i e^{-E_i/kT}} \tag{14}$$

and the components of the magnetic moments for these levels are

$$\mu(\Gamma_{3,4}) = \mp \frac{1}{2} g_z \mu_B \quad ,$$

$$\mu(\Gamma_2^i) = \mp \frac{g \mu_B}{2} \frac{g \mu_B H_z}{[(g \mu_B H_z)^2 + (2\Delta')^2]^{1/2}} \quad , \tag{15}$$

where $g = 2 g_J \langle \Gamma_2^{(2)} | J_z | \Gamma_2^{(1)} \rangle$ and where $2\Delta'$ is the splitting at $H = 0$ between the two Γ_2 levels.

The magnetization per ion for $\vec{H} \parallel \vec{b}$ is more complicated but can again be calculated directly from the partition function as we do below in the LiErF$_4$.

For $\vec{H} \parallel \vec{c}$, the analysis of the $\Gamma_{3,4} \leftrightarrow \Gamma_{3,4}$ transition (noted $1 \leftrightarrow 2$ in Fig. 6) determines the g_z value and

TABLE II. Values for the best-fit parameters obtained in LiHoF$_4$ from the frequency dependences of the resonance lines. The values of several of these parameters obtained from other works (Refs. 4, 7, 8, 13, and 23) are included for comparison.

	g_z	$\left[\lambda - \dfrac{4\pi N_c}{V}\right]M_0$ (kG)	$\dfrac{4\pi}{3}N_c$	Θ_C (K)	E_1 (GHz)	E_2 (GHz)	$\langle\Gamma_2^2|J_z|\Gamma_1^1\rangle$	$|\langle\Gamma_{3,4}|J_x|\Gamma_2^1\rangle|$
Sample 1	14.1 ±0.2	1.5 ±0.2	0.23×4π	1.9 ±0.1	215	···	4.75 ±0.2	···
Sample 2	14.1 ±0.2	1.9 ±0.2	0.21×4π	2.0 ±0.1	217	···	4.85 ±0.1	···
Sample 3	14 ±0.2	0.3 ±0.2	4π/3	1.85 ±0.1	220	694	4.85 ±0.1	2.3
LiYF$_4$:Ho^{3+} Ref. 4	13.3 ±0.1	···	···	···	204	714	4.6 ±0.1	2.3 ±0.1
Susceptibility Ref. 7	13.4	···	···	2.0 ±0.2	188	815	4.71	2.43
Optical suscept. Ref. 8	13.8 / 13.6 ±0.2	···	several crystals	1.55	222	699	···	···
Optical Ref. 13	13.79	···	···	···	240	780	4.74	2.31
Susceptibility Ref. 23	13.95 ±0.15	···	···	1.65	217	···	···	···

the λ and Θ_C constants. The analysis of the $\Gamma_{3,4} \leftrightarrow \Gamma_2$ transitions (noted $1\leftrightarrow3, 2\leftrightarrow3, 1\leftrightarrow4$ in Fig. 6) gives the positions in energy of the two Γ_2 singlets E_1,E_2 and also the matrix element $\langle\Gamma_2^{(2)}|J_z|\Gamma_2^{(1)}\rangle$ which governs the field dependence of the Γ_2 singles.

For $\vec{H}\parallel\vec{b}$, we determine, from the study of the $\Gamma_{3,4} \leftrightarrow \Gamma_2$ transitions, the matrix element $|\langle\Gamma_2^{(1)}|J_x|\Gamma_{3,4}\rangle|$. The calculated curves for the best-fit parameters are shown in Figs. 6 and 7, respectively.

The values of these parameters are given in Table II and are compared with other results.[4,7,8,13,23] The low-temperature behavior in LiHoF$_4$ is described by the fundamental doublet with $g_z = 14.1 \pm 0.2$. If there were no excited states close by, the material would be Ising-like, the same as LiTbF$_4$. The existence of the first excited state at 10.5 K limits the range of temperatures over which the Ising description can be applied. For $\vec{H}\perp\vec{c}$ the existence of couplings between this state and the fundamental doublet limits the Ising-like description. The dipolar forces are predominant in the contribution to Θ_C.[4,5,20] This system can consequently be described as dipolar and Ising-like for low temperatures provided that no magnetic field is applied perpendicular to the $\vec{c}$ axis. The critical properties do not seem to be affected by the existence of the first excited state.[22,23]

C. LiErF$_4$

Three single crystals of LiErF$_4$ were used. The first two crystals were parallelepipedic (samples 1,2) and the third spherical (sample 3).

The hyperfine structures due to the different isotopes of Er^{3+} are not resolved for any temperature or frequency.

The angular dependences of the resonance lines in the (c,a) and (a,a) planes were studied. Figure 9 shows the angular dependence in the (a,a) plane. The resonance lines show an anisotropy in the basal plane with a periodicity of 90°. Similar results had been observed on LiYF$_4$:Ho^{3+} on the angular dependences in this plane.[25]

Figures 10–12 show the frequency field dependence of the observed resonances for the magnetic field along the $\vec{c}$ axis and along the two directions in the basal plane for which the angular dependence (Fig. 9) shows a maximum and a minimum of the position in field of the resonance line.

In these figures, we observe that several signals extrapolate at zero frequency for zero magnetic fields. These resonances correspond to transitions between doublet components. Several lines extrapolate at 545 GHz for zero magnetic field and correspond to transi-
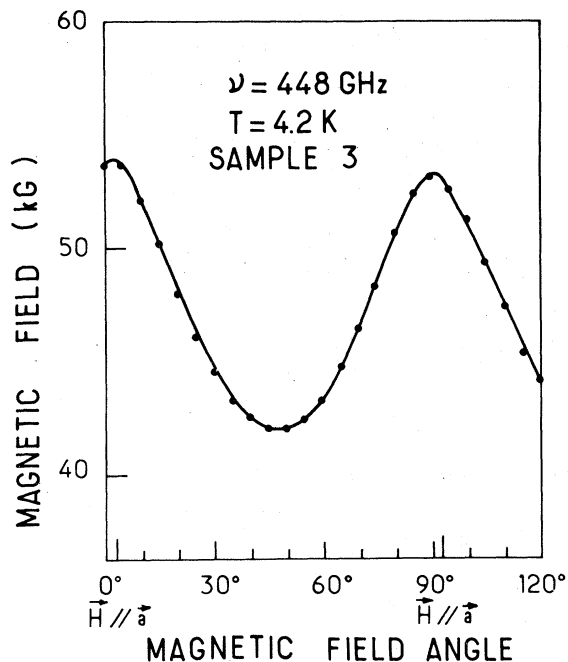
FIG. 9. Angular dependence of the resonance 1 ↔ 2 at
448 GHz for $\vec{H}\perp\vec{c}$ in LiErF$_4$ (sample 3). Dots, experiment;
continuous line, a guide to the eye.

tions between two levels 545 GHz apart.

Moreover, two resonances (noted with crosses in
Figs. 10–12) were observed at a given field at a fre-
quency which is almost exactly twice the frequency of
the resonance lines noted 1 ↔ 2. This leads us to the
following analysis: the ground term (2J + 1)fold de-
generate $^4I_{15/2}$ of the Kramers ion Er^{3+} (4f^{11}), is split
into eight doublets

$$^4I_{15/2} \rightarrow 4\Gamma_{5,6} + 4\Gamma_{7,8} .$$

From the spectroscopic[13] and the susceptibility
measurements[7] we know the lowest levels. The fun-
damental level is a $\Gamma_{5,6}$ doublet and the first excited
state a $\Gamma_{7,8}$ doublet at 18 cm^{-1}. In our experiment,
we observe only the transitions between these two
levels. However, the second excited level $\Gamma_{5,6}$ and
the third excited level $\Gamma_{7,8}$ must be taken into ac-
count for the calculation of the energy levels.

The magnetic field dependence of these levels can
be obtained from the Zeeman Hamiltonian (11) with
$g_J = \frac{6}{5}$ and from the knowledge of the wave functions
of the levels.[7,13]

The energy levels are calculated numerically from
the diagonalization of the secular equation (12), con-
sidering the four lowest doublets. The general struc-

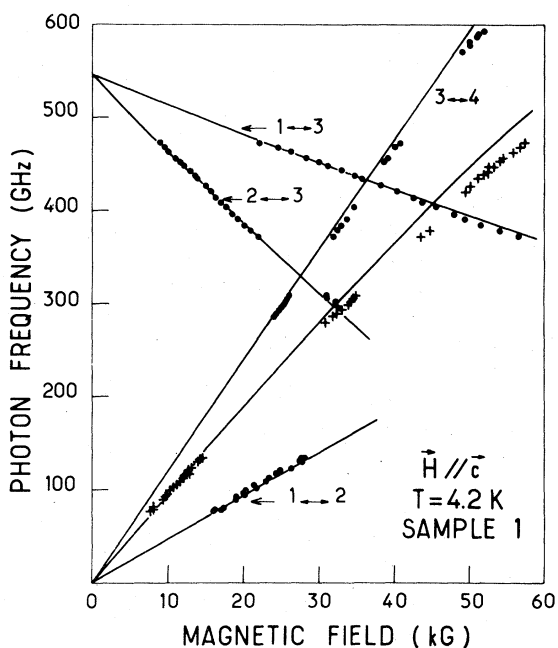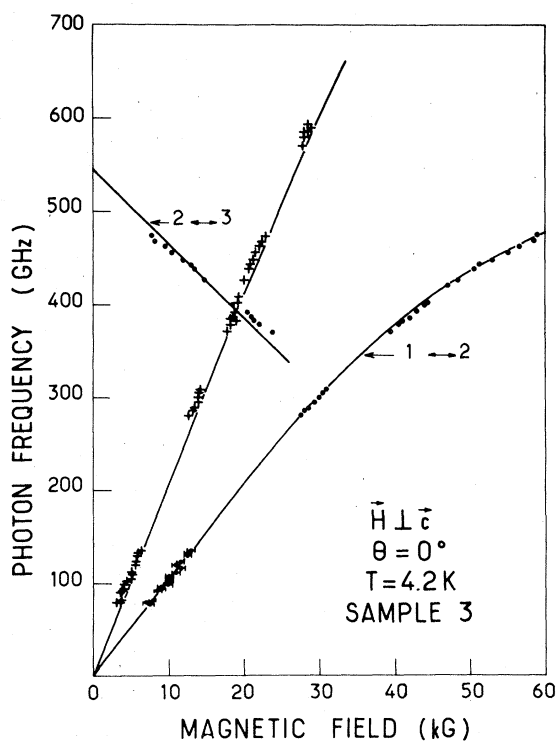

FIG. 10. Frequency vs magnetic field of the resonances
for $\vec{H}\parallel\vec{c}$ in LiErF$_4$ (sample 1). Resonance 1 ↔ 2 indicates
the transition between the two levels of the fundamental
doublet. Resonances 1 ↔ 3 and 2 ↔ 3 indicate transition
between these levels and a level of the first excited doublet.
Resonance 3 ↔ 4 indicates the transition between the two
levels of this first excited doublet (see Fig. 13). Dots, ex-
periment; continuous line, theory.

FIG. 11. Frequency vs magnetic field of the resonances
for $\vec{H}\perp\vec{c}$ and $\theta = 0°$ in LiErF$_4$ (sample 3). The resonances
are indicated with the same notation as in Fig. 10. Dots, ex-
periment; continuous line, theory.

FIG. 12. Frequency vs magnetic field of the resonances for $\vec{H} \perp \vec{c}$ and $\theta = 45°$ in LiErF$_4$ (sample 3). The resonances are indicated with the same notation as in Fig. 10. Dots, experiment; continuous line, theory.
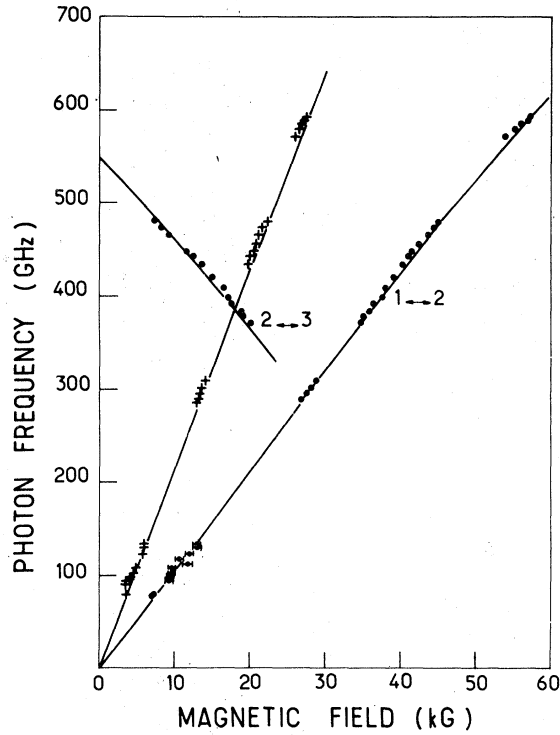
ture of the wave functions of these levels is

$$|\Gamma_{5,6}\rangle = \alpha_1 e^{\pm\beta_{1J}}|\pm\tfrac{13}{2}\rangle + \alpha_2 e^{\pm\beta_{2J}}|\pm\tfrac{5}{2}\rangle$$
$$+ \alpha_3 e^{\pm\beta_{3J}}|\mp\tfrac{3}{2}\rangle + \alpha_4 e^{\pm\beta_{4J}}|\pm\tfrac{11}{2}\rangle ,$$

$$|\Gamma_{7,8}\rangle = \alpha'_1 e^{\pm\beta'_{1J}}|\pm\tfrac{15}{2}\rangle + \alpha'_2 e^{\pm\beta'_{2J}}|\pm\tfrac{7}{2}\rangle$$
$$+ \alpha'_3 e^{\pm\beta'_{3J}}|\mp\tfrac{1}{2}\rangle + \alpha'_4 e^{\pm\beta'_{4J}}|\mp\tfrac{9}{2}\rangle .$$

$$(16)$$

The resonance lines are shifted in field due to the local magnetic field related to the external magnetic field through the expression

$$H = H_0 + \alpha M_{\text{mass}} , \quad (17)$$

where M_{mass} is the magnetization per gram. The value of α is taken from susceptibility measurements.[9]

The magnetization per ion is calculated taking into account the four lowest doublets by

$$M_{\text{ion}} = kT\frac{\partial(\ln Z)}{\partial H} , \quad (18)$$

where $Z = \sum_n e^{-En/kT}$ is the partition function.

The field dependence of the levels is shown in Fig. 13 for $\vec{H} \| \vec{c}$ and for the two directions in the $\vec{c}$ plane corresponding to Figs. 11 and 12.

For $\vec{H} \| \vec{c}$, we determine from the transition $1 \leftrightarrow 2$, the g value of the fundamental doublet and from transitions $1 \leftrightarrow 3, 1 \leftrightarrow 4$, and $3 \leftrightarrow 4$ the g value of the first excited state and the position in zero field of the

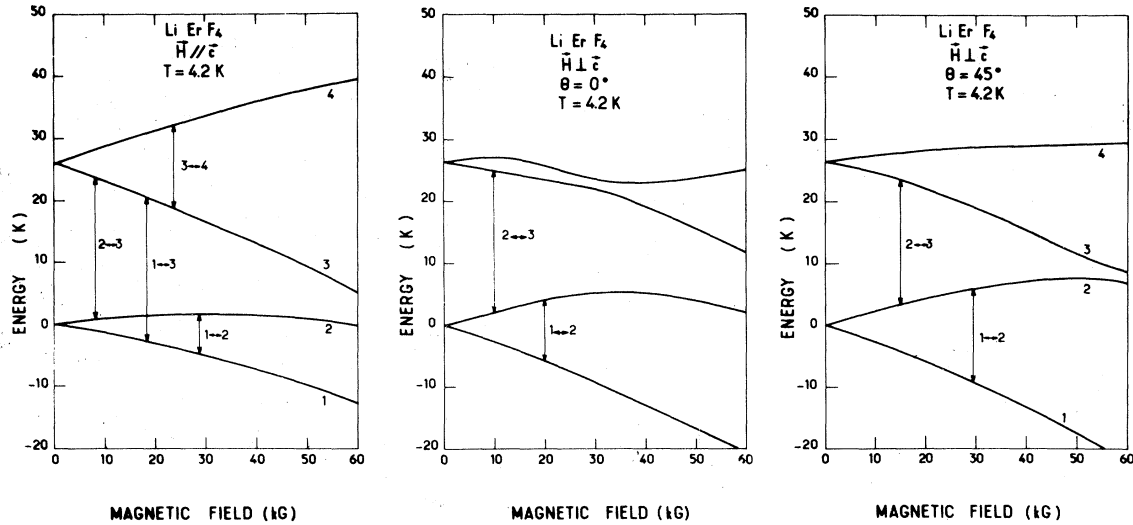FIG. 13. Scheme of the calculated energy levels in LiErF$_4$. The different transitions are indicated.

TABLE III. Values for the best-fit parameters obtained in LiErF$_4$ from the frequency dependences of the resonance lines. The values of several of these parameters obtained from other works (Refs. 7, 9, and 13) are included for comparison.

	g_{1c}	g_{2c}	α	$\frac{4\pi}{3}N_c$	E_1 (Ghz)	E_2 (GHz)	$\langle\Gamma^2_{5,6}|J_z|\Gamma^1_{5,6}\rangle$
Samples 1,2 $\vec{H}\parallel\vec{c}$	3.7 ±0.2	9.1 ±0.2	−28.6	1.66 × 4π	546	700	3.28
Susceptibility Ref. 7	3.1	8.4	· · ·	· · ·	564	920	3.28
Susceptibility Ref. 9	3.5	· · ·	−40.7	4π/3	· · ·	· · ·	· · ·
Optical Ref. 13	4.2	7.9	· · ·	· · ·	540	600	3.09
	$g_{1\perp}$	$g_{2\perp}$	$\alpha_\perp$	$\frac{4\pi}{3}N_c$	E_1	E_2	$|\langle\Gamma^1_{5,6}|J_x|\Gamma^1_{7,8}\rangle|$
Sample 3 $\vec{H}\perp\vec{c}$	8.7 ±0.2	4.6 ±0.2	−23.0	· · ·	546	700	2.69
Susceptibility Ref. 7	8.2	4.6	· · ·	· · ·	564	920	2.24
Susceptibility Ref. 9	9.2	· · ·	−23.0	4π/3	· · ·	· · ·	· · ·
Optical Ref. 13	7.8	2.05	· · ·	· · ·	540	600	1.57

two excited levels E_1,E_2. The values of the matrix elements $\langle\Gamma^1_{5,6}|J_z|\Gamma^2_{5,6}\rangle$, $\langle\Gamma^1_{7,8}|J_z|\Gamma^2_{7,8}\rangle$ and the g values for the two upper doublets are taken from Ref. 7. The best fit of these parameters is given in Table III and compared with other results.

For $\vec{H}\perp\vec{c}$, the g value of the fundamental doublet and the coupling $\langle\Gamma^1_{5,6}|J_x|\Gamma^1_{7,8}\rangle$ are determined from transition $1\rightarrow2$. The g value of the first excited doublet is determined from transition $2\rightarrow3$. The g values of the other doublets and other couplings are taken as in Ref. 7. The values of these parameters are given in Table III. The calculated curves with these parameters are shown in Figs. 10−12.

The low-temperature behavior in LiErF$_4$ is described by the fundamental doublet $g_{1z}=3.7$ and $g_{1\perp}=8.7$. These values are rather different from those of Refs. 7 and 12 but are close to those obtained from susceptibility measurements at low temperatures.[9]

LiErF$_4$ is a XY dipolar antiferromagnet ($g_{1\perp}/g_{1z}=2.35$), whereas LiTbF$_4$ and LiHoF$_4$ are Ising dipolar ferromagnets. The dipolar forces and the exchange forces are of the same order.[9] It seems therefore quite interesting to study the critical param-

eters of LiErF$_4$ and compare them with those obtained in LiTbF$_4$ and LiHoF$_4$.

Besides the main resonances, we observe in Figs. 10−12 transitions at twice the energy of that noted $1\rightarrow2$ in these figures. We attribute these resonance lines to transitions between the levels of two neighbor spins coupled by dipolar forces.

The Hamiltonian for the systems of two spins 1 and 2 is, considering only the fundamental doublet ($S_1=\frac{1}{2},S_2=\frac{1}{2}$)

$$H_{12}=\mu_B(\vec{H}\cdot\vec{g}\cdot\vec{S}_1)+\mu_B(\vec{H}\cdot\vec{g}\cdot\vec{S}_2)+\vec{S}_1\cdot\vec{D}\cdot\vec{S}_2 , \quad (19)$$

with

$$D^{\alpha\beta}_{12}=\frac{\mu_B^2 g^{\alpha\alpha}g^{\beta\beta}}{r_{12}^3}\left(\delta_{\alpha\beta}-\frac{3r^\alpha_{12}r^\beta_{12}}{r_{12}^2}\right) , \quad (20)$$

where $\alpha=x,y,z$. $g^{\alpha\alpha}$ and $g^{\beta\beta}$ are the g values of the fundamental doublet. r_{12} the distance between the spins 1 and 2.

Taking into account only the secular part of the dipolar interaction[29] the energy levels can be easily calculated. The levels are characterized by the total spin $\vec{S}=\vec{S}_1+\vec{S}_2$ and the allowed transitions are those with

$\Delta S_Z = \pm 1$. The effect of the nonsecular part of the dipolar interaction is to mix these states, and it is then possible to observe transitions $\Delta S_Z = \pm 2$ at a frequency almost exactly double that of the $\Delta S_Z = \pm 1$ transitions.[29]

In LiTbF$_4$, similar resonances cannot be observed because $g_\perp = 0$, and consequently the nonsecular part of the dipolar interaction is zero.

In LiHoF$_4$, the resonance observed at frequency sum of the $1 \leftrightarrow 2$ and $1 \leftrightarrow 3$ transition, can also be attributed to a transition between the levels of two nearest-neighbor spins and considering, in this case, the three lowest levels of the Ho^{3+} ion.

III. SUMMARY

The g factor and the Δ splitting of the fundamental doublet of LiTbF$_4$ are determined directly from EPR experiments in a large range of frequencies and magnetic fields. The local field around the Tb^{3+} ion is determined and the Curie constant calculated. These parameters describe the magnetic behavior of the crystal at low temperatures.

The temperature dependence of the linewidth of the resonance line is observed for $1.4 < T < 25$ K and analyzed in terms of the theory of line moments.

In LiHoF$_4$, we determine the g factor of the fundamental doublet, the energy of the first two excited states, and the coupling between all these levels in a magnetic field parallel and perpendicular to the tetragonal $\bar{c}$ axis. The local field and the Curie constant are also determined. The temperature dependence of the linewidths was observed.

LiTbF$_4$ and LiHoF$_4$ are quasi-ideal examples of dipolar Ising ferromagnets. Small deviations from the ideal behavior are produced by the single-ion parameters, which are determined in this work.

The g factors, and the couplings between the first two doublets are determined in LiErF$_4$ which is described as an XY dipolar antiferromagnet.

Some transitions observed in LiErF$_4$, attributed to transitions between the levels of two neighbor ions, are analyzed.

ACKNOWLEDGMENTS

*Also, Université Pierre et Marie Curie (Paris VI).

†Laboratoire Associé au Centre National de la Recherche Scientifique.

[1]E. P. Chiklis, C. S. Naiman, R. C. Folweiler, D. R. Gabbe, H. P. Jenssen, and A. Linz, Appl. Phys. Lett. 19, 119 (1971).

[2]J. P. Sattler and J. Nemarich, Phys. Rev. B 4, 1 (1971).

[3]I. Laursen and L. M. Holmes, J. Phys. C 7, 3765 (1974).

[4]J. Magariño, J. Tuchendler, J. P. D'Haenens, and A. Linz, Phys. Rev. B 13, 2805 (1976).

[5]L. M. Holmes, T. Johansson, and H. J. Guggenheim, Solid State Commun. 12, 993 (1973).

[6]L. M. Holmes, J. Als-Nielsen, and H. J. Guggenheim, Phys. Rev. B 12, 180 (1975).

[7]P. E. Hansen, T. Johansson, and R. Nevald, Phys. Rev. B 12, 5315 (1975).

[8]A. H. Cooke, D. A. Jones, J. F. A. Silva, and M. R. Wells, J. Phys. C 8, 4083 (1975); J. E. Battison, A. Kaster, M. J. M. Leask, J. B. Lowry, and B. M. Wanklyn, J. Phys. C 8, 4089 (1975).

[9]P. Beauvillain, J. P. Renard, and P. E. Hansen, J. Phys. C 10, L709 (1977).

[10]S. K. Misra and J. Felsteiner, Phys. Rev. B 15, 4309 (1977).

[11]P. Beauvillain and J. P. Renard (unpublished).

[12]H. P. Christensen, Phys. Rev. B 17, 4060 (1978).

[13]H. P. Christensen (unpublished).

[14]A. I. Larkin and D. E. Khemel'nitskii, Sov. Phys. JETP 29, 1123 (1969).

[15]A. Aharony, Phys. Rev. B 8, 3363 (1973).

[16]L. M. Holmes, F. Hulliger, H. J. Guggenheim, and J. P. Maita, Phys. Lett. A 50, 163 (1974).

[17]G. Ahlers, A. Kornblit, and H. J. Guggenheim, Phys. Rev. Lett. 34, 1227 (1975).

[18]J. Als-Nielsen, L. M. Holmes, and H. J. Guggenheim, Phys. Rev. Lett. 32, 610 (1974).

[19]J. Als-Nielsen, L. M. Holmes, F. Krebs Larsen, and H. J. Guggenheim, Phys. Rev. B 12, 191 (1975).

[20]J. Als-Nielsen, Phys. Rev. Lett. 37, 1161 (1976).

[21]J. A. Griffin, J. D. Litster, and A. Linz, Phys. Rev. Lett. 38, 251 (1977).

[22]P. Beauvillain, J. P. Renard, I. Laursen, and P. J. Walker, J. Phys. (Paris) 39, C6-745 (1978).

[23]P. Beauvillain, J. P. Renard, I. Laursen, and P. J. Walker, Phys. Rev. B 18, 3360 (1978).

[24]J. Magariño, J. Tuchendler, and P. E. Hansen, Physica (Utrecht) B 86-88, 1223 (1977).

[25]J. Magariño and J. Tuchendler (unpublished).

[26]K. Kambe and T. Usui, Prog. Theor. Phys. (Kyoto) 8, 302 (1952).

[27]M. McMillan and W. Opechowski, Can. J. Phys. 38, 1168 (1960).

[28]I. Svare and G. Seidel, Phys. Rev. 134, A172 (1960).

[29]A. Abragam and B. Bleaney, Electron Paramagnetic Resonance of Transition Ions, (Clarendon, Oxford, 1970).